Pulmonary exposure to cellulose nanocrystals caused deleterious effects to reproductive system in male mice

Mariana T. Farcas, Elena R. Kisin, Autumn L. Menas, Dmitriy W. Gutkin, Alexander Star, Richard S. Reiner, Naveena Yanamala, Kai Savolainen & Anna A. Shvedova

Published online: 24 Aug 2016.

Submit your article to this journal ⬀

View related articles ⬀

View Crossmark data ⬀

Taylor & Francis
Taylor & Francis Group

Pulmonary exposure to cellulose nanocrystals caused deleterious effects to reproductive system in male mice

Mariana T. Farcas[a], Elena R. Kisin[a], Autumn L. Menas[a], Dmitriy W. Gutkin[b], Alexander Star[c], Richard S. Reiner[d], Naveena Yanamala[a], Kai Savolainen[e], and Anna A. Shvedova[a,f]

[a]Exposure Assessment Branch/NIOSH/CDC, Morgantown, West Virginia, USA; [b]Department of Pathology, University of Pittsburgh Medical Center, Pittsburgh, Pennsylvania, USA; [c]Department of Chemistry, University of Pittsburgh, Pittsburgh, Pennsylvania, USA; [d]Forest Products Laboratory, USDA Forest Service, Madison, Wisconsin, USA; [e]Finnish Institute of Occupational Health, Helsinki, Finland; [f]Department of Physiology & Pharmacology, School of Medicine/WVU, Morgantown, West Virginia, USA

ABSTRACT

Over the past several years there has been an increased number of applications of cellulosic materials in many sectors, including the food industry, cosmetics, and pharmaceuticals. However, to date, there are few studies investigating the potential adverse effects of cellulose nanocrystals (CNC). The objective of this study was to determine long-term outcomes on the male reproductive system of mice upon repeated pharyngeal aspiration exposure to CNC. To achieve this, cauda epididymal sperm samples were analyzed for sperm concentration, motility, morphological abnormalities, and DNA damage. Testicular and epididymal oxidative damage was evaluated, as well as histopathology examination of testes. In addition, changes in levels of testosterone in testes and serum and of luteinizing hormone (LH) in serum were determined. Three months after the last administration, CNC exposure significantly altered sperm concentration, motility, cell morphology, and sperm DNA integrity. These parameters correlated with elevated proinflammatory cytokines levels and myeloperoxidase (MPO) activity in testes, as well as oxidative stress in both testes and epididymis. Exposure to CNC also produced damage to testicular structure, as evidenced by presence of interstitial edema, frequent dystrophic seminiferous tubules with arrested spermatogenesis and degenerating spermatocytes, and imbalance in levels of testosterone and LH. Taken together, these results demonstrate that pulmonary exposure to CNC induces sustained adverse effects in spermatocytes/spermatozoa, suggesting male reproductive toxicity.

During the past decades, there has been an increased market demand for development of novel applications for cellulosic nanomaterials (CN) (Cherian et al., 2011). The physicochemical and mechanical properties make cellulose an excellent, reliable source for manufactured goods in many sectors for use in the paper and food industry, cosmetics, biomedicine, and pharmaceutical production (Wegner et al., 2013). Cellulose, the most abundant organic compound on Earth, and its derivatives are considered to be natural, biocompatible, biodegradable, and renewable materials that are generally considered safe for humans and the environment (Wegner et al., 2013).

Despite the European and U.S. government agencies supporting the development of nanotechnology and innovative nanoscale products (Goldman and Coussens, 2005), the novelty of certain nanomaterials may lead to unexpected interactions with biological and environmental systems (Buzea et al., 2007; Kermanizadeh et al., 2016). Specifically, during the manufacturing (e.g., embedding or compounding with polymers) and their final disposal, CN may be released into the air and therefore pose risk to workers. Further, when incorporated into consumer's products like cosmetics, drug powder form, and condiments, and in surgical or postoperative procedures, the general population may be at risk (Peng et al., 2011; Brown et al., 2013; Zhang et al., 2016). Because of their nanoscale features, inhalable nanomaterials are easily deposited deeper in the lung compared to larger particles (Buzea et al., 2007; Oberdörster et al., 2015). Further, the high aspect ratio of CN along with fibrous nature may impose safety concerns (Shvedova et al., 2014; Cyphert et al., 2016; Snyder-Talkington et al., 2016).

To date, limited data are available describing adverse health outcomes elicited by cellulose nanocrystals (CNC). Clift and colleagues (2011) indicated that CNC exposure induced a significant concentration-dependent cytotoxicity and proinflammatory response in a coculture model of human lung cells. Catalan et al. (2015) reported a 55% cytotoxic effect of CNC and nano-scale microcrystalline CN in human bronchial epithelial cells. Recently, Yanamala et al. (2014) noted that acute pharyngeal aspiration exposure to respirable CNC (dose of 50–200 µg/mouse) produced pulmonary inflammation and damage, accelerated oxidative stress accompanied by increase in proinflammatory cytokines release seen in the bronchoalveolar lavage fluids (BALF) and lungs of C57BL6 mice. In our latest study Shvedova et al. (2016) found that pulmonary exposure to CNC induced long-term outcomes that led to pulmonary inflammation, oxidative stress, and collagen accumulation following 3 mo post treatment. Further, Stefaniak et al. (2014) demonstrated that cellulose nanofibrils and CNC were able to generate hydroxyl radicals in vitro with higher levels attributed to CNC effects. Excessive generation of reactive oxygen species (ROS) was reported to play a vital role in male infertility (Oliva et al., 2001). ROS may stimulate release of apoptosis-inducing factor (AIF), leading to high frequency of a single- and double-stranded DNA breaks, base oxidation, and chromatin cross-linking (Agarwal et al., 2014), producing a detriment in terms of sperm integrity and male infertility (Aitken and Roman, 2008). In addition, elevated ROS levels were found to induce sperm mitochondrial membrane damage, release of cytochrome c, activation of caspase pathways, and apoptotic signaling (Makker et al., 2009). Further, in a clinical case study, a high 10-fold rate of developing testicular cancer was reported in sons of men working in the wood-processing industry compared to males in the general populations (Knight and Marrett, 1997).

Infertility is a major problem in industrialized countries, not only affecting birth rates but also producing severe psychosocial distress in men (Greil et al., 2010). Sharlip et al. (2002) indicated that 15% of all couples in the United States are infertile, and the male factor was reported to be responsible in 25% of the cases. During the past four decades, there has been increased attention to male reproductive problems produced by occupational exposures in humans (Jouannet et al., 2001; Phillips and Tanphaichitr, 2008). Previous studies showed that numerous nanomaterials, such as metal-based (TiO_2) and carbon-based particles (carbon black, multiwalled carbon nanotubes) and nanoparticle-rich diesel exhaust, have the ability to penetrate blood–testis and placental barriers, thus, exerting detrimental effects on endocrine and reproductive systems (Iavicoli et al., 2013; Liu et al., 2016). Hence, considering both the growing volume of CNC manufacturing and launching of novel products in the U.S. market, it is imperative to address whether exposure to inhalable CNC might mediate male reproductive toxicity (Oliva et al., 2001; Cherian et al., 2011). The objective of this study was to assess whether pulmonary exposure of C57BL/6 mice to respirable CNC produced long-term outcomes in the male reproductive system.

Materials and Methods

Preparation and Administration of CNC

Wood-pulp-derived cellulose nanocrystals, as freeze dried (powder form) samples, were a gift from Forest Products Laboratory (FPL, U.S. Forest Service, Madison, WI). Average dimensions of CNC used in the study were published previously by Shvedova et al. (2016): 158 ± 97 nm length, 54 ± 17 nm width and 149.8 ± 2.6 nm hydrodynamic diameter. Prior to animal exposures, the CNC stock suspensions in USP grade water, were sonicated for 2 min with a probe sonicator (Branson Sonifier 450, 10 W continuous output), and sterilized by autoclaving. Endotoxin levels in CNC stock solution were below the detection limit (0.01 endotoxin units [EU]/ml) as assessed by a *Limulus* amebocyte lysate (LAL) chromogenic endpoint assay kit (Hycult Biotech, Inc., Plymouth Meeting, PA). Mice were exposed to a cumulative CNC dose of 240 µg/mouse. Specifically, human equivalent workplace exposure to a deposited cumulative concentration of 240 µg cellulose may be achieved in approximately 42 working days at allowable exposure concentration limits defined by the Occupational Safety and

Health Administration (OSHA; 5 μg/m^3 of cellulose). Calculations were performed using the formula published previously by Yanamala et al. (2014).

Animals

Experiments were conducted with adult male C57BL/6 mice (n = 40) (Jackson Laboratories, Bar Harbor, ME), aged 7–8 wk and weighing 20 ± 1.9 g when used. The animals were maintained in individual cages, receiving HEPA-filtered air, and supplied with nutritionally adequate pelleted food (certified feed 7913, Harlan Teklad, Indianapolis, IN) and water ad libitum. Beta Chips (Northeastern Products Corp., Warrensburg, NY) were utilized for bedding and changed weekly. Animals were acclimated in the animal facility for at least 1 wk before use. All animals were housed in the Association for Assessment and Accreditation of Laboratory Animal Care (AAALAC) International-accredited National Institute of Occupational and Safety Health (NIOSH) animal facility. All experimental procedures were conducted in accordance with guidelines and policy set forth by the Institute of Laboratory Animal Resources, National Research Council and approved by the NIOSH Institutional Animal Care and Use Committee (IACUC).

General Experimental Design

Animals were divided randomly into two groups: control (n = 20) and CNC-exposed group (n = 20). Mice were administered either CNC (40 μg/mouse/d) or vehicle (USP sterile water, Hospira, Inc., USA) by pharyngeal aspiration. Briefly, after anesthesia with a mixture of ketamine and xylazine (Phoenix, St. Joseph, MO) (62.5 and 2.5 mg/kg intraperitoneal [ip] in the abdominal area), the mouse was placed on a board in a near-vertical position and the animal's tongue was extended with lined forceps. A suspension of cellulose (40 μg/mouse/d, twice a week, for 3 wk) was placed posterior in the throat and the tongue was held until the suspension was aspirated into the lungs. Mice were sacrificed 3 mo following pulmonary exposure to CNC to assess reproductive outcomes in males. This time point was selected based upon findings from Shvedova et al. (2016), who showed significant respiratory damage and impairment of lung functions. At the time of euthanasia, following ip injection of pentobarbital, blood samples were drawn from the inferior vena cava and allowed to clot at 4 °C for 1.5 hr then pelleted. Serum was collected after centrifugation (15 min; 1700 × g; 4 °C) and stored at –80°C until assayed for testosterone, luteinizing hormone (LH), and cytokines levels. The testes were either stored at –80°C until processed for testosterone measurements, cytokines responses, and biomarkers of oxidative stress, or used for histologic examination. The epididymis was excised and trimmed to remove excess tissue and fat. The right epididymis was processed for semen analysis (sperm density, motility, and morphology evaluation), while the left epididymis was employed for either assessment of sperm DNA fragmentation or oxidative stress measurements.

Semen Collection and Sperm Analysis

Sperm Count

The right epididymis, separated from the testicle, was further processed for sperm counts as described previously (Kisin et al., 2014). Briefly, in a petri dish containing prewarmed M16 medium (Sigma-Aldrich, St. Louis, MO), epididymal cauda was minced with scissors and then incubated at 37°C for 5 min to allow spermatozoa to disperse. Sperm concentration was assessed using a Neubauer hemocytometer chamber (Hausser Scientific, Horsham, PA). Cell counts were repeated twice for each sample. The sperm cell suspension was further processed for motility and morphology evaluation as described next.

Sperm Motility

Approximately 500 cells per slide were tracked for motility assessment by scoring the number of all motile and nonmotile sperm within the same field using a hemocytometer chamber. The assessment of the motile sperm fraction was defined as the mean number of motile sperm × 100/total number of sperm.

Sperm Morphology

Eosin Y staining (Leica Microsystems, Inc., Buffalo Grove, IL) was used for evaluation of sperm cells with normal morphology and cells displaying abnormalities in head, midpiece, and tail, as described previously (Pereira et al., 1981). Briefly, the sperm suspension was mixed with Eosin Y (9:1 ratio) and incubated for 30 min at room temperature. A drop of sperm suspension was smeared on the slide, air-dried, and mounted with low-viscosity mounting medium. At least 500 spermatozoa were examined per each slide using bright-field microscopy (1000× magnification) (Olympus Provis, B&B Microscopes, USA).

Sperm DNA Fragmentation Index (DFI)

The genetic integrity of the spermatozoan was assessed by the sperm chromatin structure assay (SCSA). The SCSA provides evaluation of 5000 cells and detection of damaged sperm DNA in sperm nuclei using flow cytometry of acridine orange-stained sperm samples (Evenson, 2013). Cell suspensions from left caudal epididymis were incubated (5 min, 37°C), filtered through a 70-µm sterile cell strainer to remove the tissues/debris to form uniform sperm cells, and centrifuged (2000 rcf, 3 min, 37°C). The supernatant was discarded; sperm cells were resuspended in 100 µl M16 medium and stored in liquid nitrogen until further processing by SCSA Diagnostics (Brookings, SD). Briefly, samples prepared according to Evenson (2013) protocol were thawed and prepared up to $1–2 \times 10^6$ sperm/ml with Tris-Na-EDTA (TNE) buffer. An aliquot of 200 µl of this sperm suspension was mixed with 400 µl of acid detergent solution and incubated for 30 s. After incubation, 1.2 ml of acridine orange (Polysciences, Inc., Warrington, PA) staining solution was added to the sample and measured by flow cytometry. Each sample was assessed in duplicate.

Preparation of Testes and Epididymis Homogenates

Testes and epididymis were dissected, weighed, and homogenized using a tissue tearor (model 985-370, Biospec Products, Inc., Racine, WI) in cold PBS (pH 7.4, 4°C). The homogenate was immediately aliquoted and stored at –80°C until used.

Total Protein Measurements

Measurement of total protein in testes and epididymis homogenates was performed by a modified Bradford assay according to the manufacturer's instructions (BioRad, Hercules, CA). Briefly, a protein dye reagent was added to the samples and incubated for 5 min. The absorbance (595 nm) was run using a Synergy H1 hybrid multimode microplate reader (BioTek Instruments, Inc., Winooski, VT), and the protein amount was calculated using bovine serum albumin as a standard.

Evaluation of Oxidative Stress Biomarkers

Oxidative damage to testes and epididymis following repeated CNC exposure was evaluated by the presence of lipid peroxidation products (HNE-His) and glutathione (GSH) in tissue homogenates. HNE-His adducts were quantified by ELISA using the OxiSelect HNE-His adduct kit (Cell Biolabs, Inc., San Diego, CA). The quantity of HNE-His adducts in protein samples were determined by comparing their absorbance (450 nm) with that of a known HNE–bovine serum albumin (BSA) standard curve using a Synergy H1 hybrid multimode microplate reader (BioTek Instruments, Inc., Winooski, VT). Depletion of GSH was assessed using ThioGlo-3 reagent (Covalent Associates, Inc., Corvallis, OR). Briefly, samples were mixed with maleimide reagent, and following 30 min of incubation, fluorescence (ex: 378 nm, em: 446 nm) was measured using a Synergy H1 hybrid multimode microplate reader (BioTek Instruments, Inc., Winooski, VT). The concentrations were calculated using L-glutathione reduced (Sigma Aldrich, St. Louis, MO) as a standard.

Histopathology of Testis Tissue

Testes were removed and fixed with 10% buffered formaldehyde. Tissues were embedded in paraffin and sectioned in the sagittal plane through the center of the organ at a thickness of 5 µm on an HM 320 rotary microtone (Carl Zeiss, Thornwood, NY). Prepared sections were stained with hematoxylin and eosin (H&E). Samples were coded to

ensure unbiased assessment and blindly evaluated by a Board-certified pathologist.

Quantification of Cytokines/Chemokine/Growth Factors

The levels of cytokines, chemokines, and growth factors in serum and testes homogenates were measured in exposed or control groups using the 23-Bio-Plex mouse cytokine assay kit (Bio-Rad, Hercules, CA). The concentrations were calculated using Bio-Plex Manager 6.1 software from standard curves.

Myeloperoxidase (MPO) Activity

Inflammatory response in testes of mice after repeated exposure to CNC was determined by measurement of myeloperoxidase (MPO) activity in homogenates using the NWLSS Myeloperoxidase Kit (Northwest Life Science Specialties, Vancouver, WA) according to the manufacturer's instructions. MPO activity was analyzed by measuring hypochlorous acid (HOCL)-dependent chlorination of β-amino acid taurine. MPO activity was normalized by the total protein content in each tissue homogenate.

Testosterone and Luteinizing Hormone Measurements

The concentration of testosterone in serum and testes was determined by a mouse enzyme-linked immunosorbent assay (ELISA) kit (BlueGene Biotech Ltd., Shanghai, China) using a monoclonal anti-testosterone antibody and a testosterone–horseradish peroxidase (HRP) conjugate. Briefly, standards, fourfold diluted serum samples, and buffer were incubated together with testosterone–HRP conjugate in precoated strips (1 h, 37°C). After incubation, wells were washed 5 times using the ELx50 automated strip washer (BioTek Instruments, Inc., Winooski, VT). The wells were then incubated with a substrate (15 min, at 37°C) under cover with aluminum foil to avoid direct light exposure. The optical density (450 nm) was determined immediately using a Synergy H1 hybrid multimode microplate reader (BioTek Instruments, Inc., Winooski, VT). The results

were calculated using Gen5 data analysis software (BioTek Instruments, Inc., Winooski, VT), based on a four-parameter logistic curve-fit regression curve. The levels of luteinizing hormone (LH) in serum were determined using a mouse ELISA kit (BlueGene Biotech Ltd., Shanghai, China) according to the manufacturer's instructions.

Statistical Analysis

Treatment-related differences in various outcomes were evaluated using Student's t-test. Results are presented as mean ± SEM. Those p values <.05 were considered statistically significant (Statistical package SigmaPlot 12.5).

Results

Animals

All mice from control and CNC-exposed groups survived the exposure without negative behavioral or adverse health outcomes. Behavioral patterns, body condition score, respiratory rate, food and water intake, defecation, urination, skin lesions, eyes or nose discharges, and perineal soiling were assessed daily by animal husbandry personnel. Weights of animals were recorded weekly, starting a day before exposure and continuing up to euthanasia. The body weight gain in exposed (4.59 ± 0.52 g) was significantly different from that of controls (7.2 ± 0.78 g).

Cauda Epididymal Sperm Analysis: Sperm Counts, Motility, Morphology, and DNA Damage

Pulmonary exposure to CNC produced a significant 40% decline in spermatozoa counts (Figure 1A) and a significant 50% decrease in motile sperm cells (Figure 1B) in exposed mice. Morphological evaluation of sperm smear indicated a significantly higher abnormality score found in mice treated with CNC compared to respective controls. In mice exposed to CNC there was a significant increase in thin and elongated head (2.67-fold), club-shaped head (1.5-fold), looping midpiece (1.57-fold), and bent midpiece (2.37-fold), as shown in Figure 2A. The DNA fragmentation index was significantly elevated,
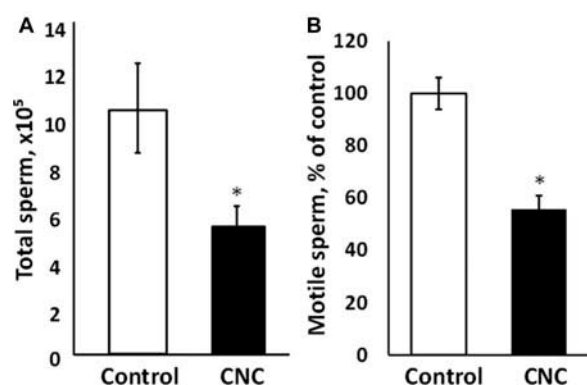
Figure 1. Epididymal sperm concentration (A) and motility (B) following pulmonary exposure to CNC. Mice were exposed twice a week for 3 consecutive weeks with a cumulative dose of 240 μg/mouse of CNC and sacrificed 3 mo following their last exposure. The values are expressed as percent of control, which is set at 100%. Mean ± SE (n = 10 mice per group). Asterisk indicates significantly different from controls ($p < .05$).

ranging from 2.61 to 3.32% in exposed mice (Figure 2B).

Oxidative Stress Markers

Assessment of testicular oxidative damage showed a significant twofold increase in HNE–protein adducts levels in exposed mice compared to controls (Figure 3A). Levels of GSH in testes were significantly reduced by 27% in CNC-treated mice (Figure 3B). In addition, exposure to respirable CNC produced significant alterations in epididymis. An 85% increase of HNE (Figure 3C) and

21% decrease in GSH levels (Figure 3D) were noted in exposed mice.

Histopathology

Microscopic evaluation of H&E-stained sections of testes in controls revealed normal architecture of seminiferous tubules and orderly spermatogenesis. However, sections of testes in the CNC-exposed group displayed interstitial edema and frequent dystrophic seminiferous tubules (20%) with arrested spermatogenesis and degenerating spermatocytes (Figures 4B–4D). There was no significant necrosis or fibrosis. Sertoli and Leydig cells were not significantly affected compared to the control. The images demonstrate dystrophic seminiferous tubules. The arrows (Figures 4B–4D) indicate cell dystrophy and arrested spermatogenesis. The changes were similar in all exposed animals, and were mild to moderate (1–2 on a scale of 3). Since the histology of testes in control animals was devoid of pathologic abnormalities, these alterations were significant.

Testosterone and LH Levels

Repeated exposure to CNC produced significant elevation in testosterone levels in testes and serum of male mice by 21 and 28%, respectively (Figures 5A and 5B). LH levels in serum were significantly reduced by 15% in exposed mice (Figure 5C).
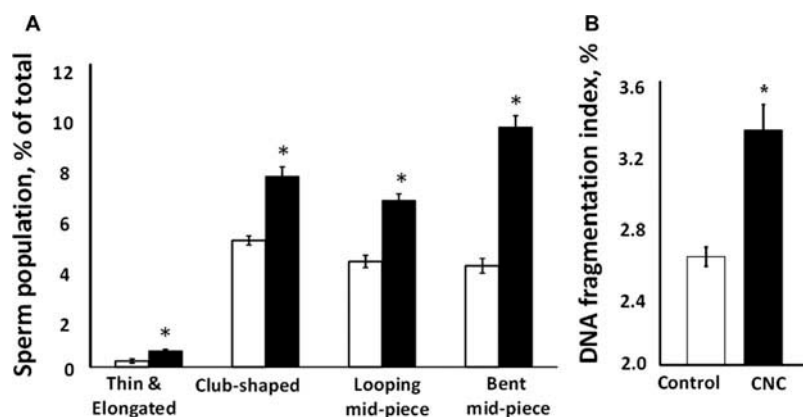
Figure 2. Morphological abnormalities of epididymal sperm (A) and DNA damage (B) following pulmonary exposure to CNC. Mice were exposed twice a week for 3 consecutive weeks with a cumulative dose of 240 μg/mouse of CNC and sacrificed 3 mo following their last exposure. (A) Data presented as percent of abnormal cells population when compared with total number of sperm. White and black bars represent control and exposed mice, respectively. (B) Data presented as percent of sperm cells containing DNA damage. Each measurement was assayed in duplicate. Mean ± SE (n = 10 mice per group). Asterisk indicates significantly different from controls ($p < .05$).
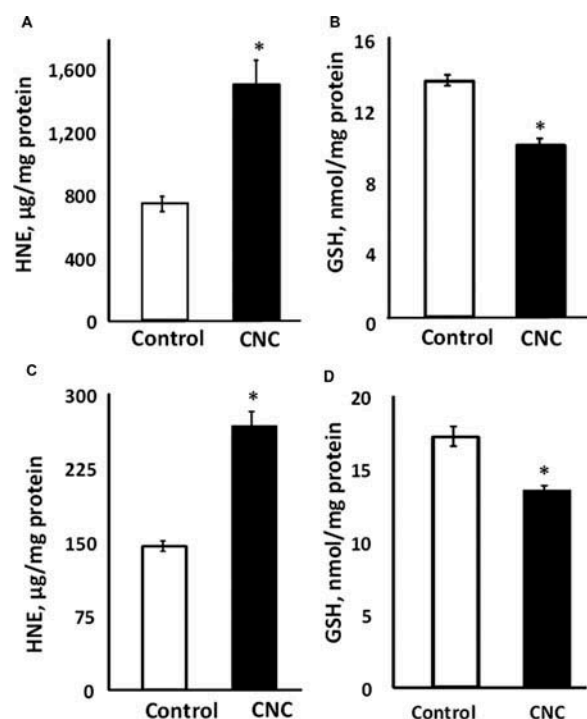
Figure 3. Oxidative stress responses in the testes (A, B) and epididymis (C, D) induced by CNC pulmonary exposure: formation of HNE-His adducts (A, C) and depletion of glutathione (GSH) (B, D). Mice were exposed twice a week for 3 consecutive weeks with a cumulative dose of 240 µg/mouse of CNC and sacrificed 3 mo following their last exposure. Each measurement was assayed in triplicate and normalized by total protein content in tissue homogenates. Mean ± SE (n = 10 mice per group). Asterisk indicates significantly different from controls (p < .05).

### MPO Activity and Cytokines/Growth Factors

Evaluation of inflammatory responses in testes 3 mo after repeated exposure to CNC showed significantly enhanced MPO activity along with increased accumulation of proinflammatory cytokines/chemokines. A significant increase in MPO (20%) was observed in CNC-exposed mice (Figure 6). Analysis of cytokines, chemokines, and growth factors levels in testes (Table 1) demonstrated significantly elevated numbers of proinflammatory cytokines and chemokines: Interleukin (IL)-1α, IL-1β, IL-2, IL-12p70, and tumor necrosis factor (TNF)-α were up-regulated by 12, 17, 23, 151 and 38%, respectively, over control. Further, a significant increase of keratinocyte chemoattractant (KC), monocyte chemoattractant protein (MCP)-1 and RANTES by 57, 22, and 105%, respectively, over control was noted. The anti-inflammatory cytokine IL-13 was

elevated by 42% in exposed mice. The levels of other cytokines (IL-5, IL-6, IL-10, IL-12(p40), IL-17, eotaxin, interferon [IFN]-γ, and macrophage inflammatory protein [MIP]-1β) were not markedly altered. To determine whether pulmonary exposure to CNC mediated systemic effects, a numbers of cytokines were measured in serum (Table 2). Data demonstrated that IL-1β, IL-2, IL-12p40, KC, MCP-1, and TNF-α were 25, 38, 43, 34, 16, and 29% higher in exposed animals, respectively. IL-4 was 62% higher in CNC-treated mice, while eotaxin, an essential chemokine, playing a role in allergic responses, was elevated by 42% after exposure.

Discussion

Shvedova et al. (2016) reported that 3 mo post repeated pulmonary CNC administration resulted in significant pulmonary inflammation, oxidative stress, and collagen accumulation in lungs. The goal of the current study was to assess whether pulmonary exposure to CNC produced male reproductive toxicity following 3 mo post recovery. The male reproductive system is susceptible to many exogenous factors that generally interfere with all stages of spermatogenesis. Iommiello et al. (2015) reported that oxidative stress and ROS are critical factors that play a role in male infertility. This is further supported by previous in vivo studies, where decreased sperm motility, DNA damage, and abnormal sperm morphology were found upon exposure to different nanoparticles (Yoshida et al., 2009; Guo et al., 2009; Gromadzka-Ostrowska et al., 2012; Kisin et al., 2014). These changes were associated with increased production of ROS. Similarly, our data demonstrated that sperm counts, motility, morphology, and sperm DNA were significantly altered in CNC-exposed mice (Figures 1 and 2). These outcomes may be attributed to peroxidative modification of lipids of sperm plasma membrane, as high levels of generated ROS render spermatozoa susceptible to oxidative injury (Griveau et al., 1995; Kodama et al., 1996). While ROS plays a vital role in normal sperm viable milieu, overproduction of those might interfere with spermatogenesis, thus affecting fertilizing function. Although testes were furnished with effective
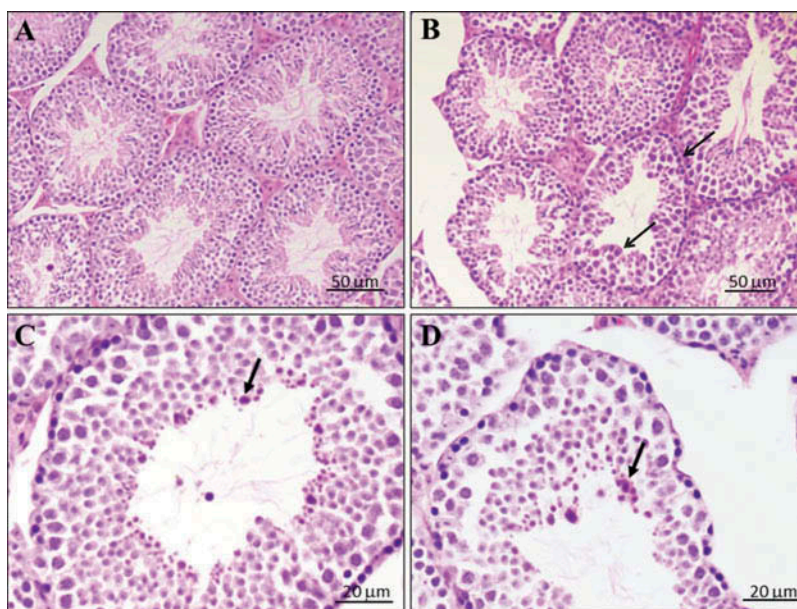
Figure 4. Representative light micrographs of H&E-stained sections from seminiferous tubule following CNC exposure. Mice were exposed twice a week for 3 consecutive weeks with a cumulative dose of 240 μg/mouse of CNC and sacrificed 3 mo following their last exposure: (A) control mice (n = 10), and (B, C, and D) CNC-exposed mice (n = 10). Arrows indicate arrested spermatogenesis and/or degenerating spermatocytes.
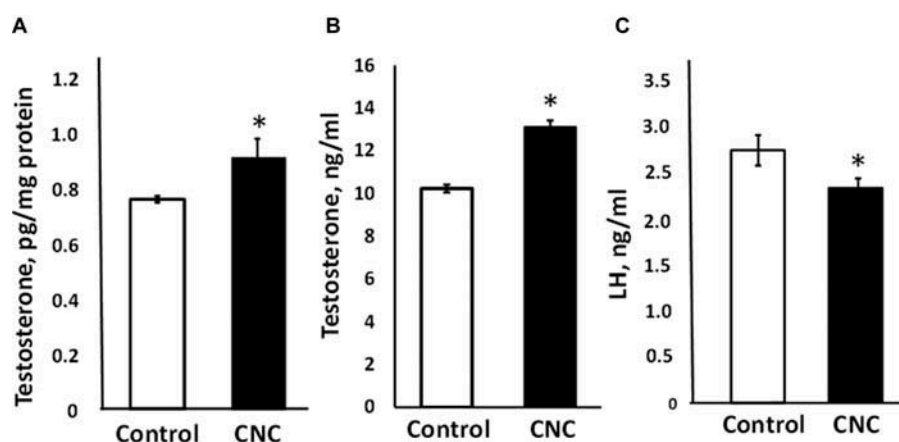

Figure 5. Testosterone levels in the testes homogenate (A) and in the serum (B), and LH (C) release in serum of mice exposed to CNC. Mice were exposed twice a week for 3 consecutive weeks with a cumulative dose of 240 μg/mouse of CNC and sacrificed 3 mo following their last exposure. Mean ± SE (n = 10 mice per group). Asterisk indicates significantly different from controls ($p < .05$).

antioxidant defense, the ability to prevent consequences of overproduction ROS during sperm formation and development as shown previously by Rajesh Kumar et al. (2002) and Shrilatha et al. (2007) may overcome these defenses.

The accumulation of lipid peroxidation products (HNE-His) was markedly elevated in testes and epididymis of mice exposed to CNC (Figure 3A and Figure 3C). This was accompanied by a decrease in GSH levels (Figure 3B and Figure 3D) upon exposure to CNC. The observed reduction in GSH may be associated with lack of ability to scavenge ROS, detoxifying formed lipid peroxides and hydrogen peroxide (H_2O_2) by glutathione peroxidases (Masella et al., 2005). Our results are in agreement with previous findings indicating that mature spermatozoa are unable to repair injury induced by ROS, due to the lack of the essential cytoplasmic enzymatic antioxidant systems required to facilitate repair (Agarwal
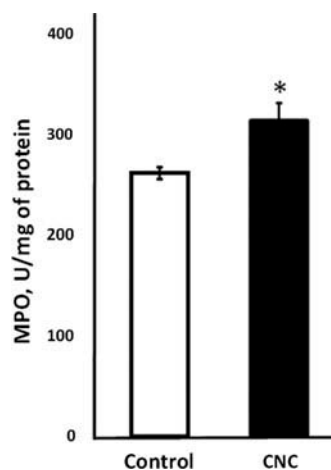
Figure 6. Inflammatory response in the testes evaluated by the changes in MPO activity following CNC exposure. Mice were exposed twice a week for 3 consecutive weeks with a cumulative dose of 240 µg/mouse of CNC and sacrificed 3 mo following their last exposure. Each measurement was assayed in triplicate and normalized by total protein content in tissue homogenates. Mean ± SE (n = 10 mice per group). Asterisk indicates significantly different from controls ($p < .05$).

Table 1. Levels (pg/mg) of cytokines, chemokines, and growth factors in the testes homogenates following CNC exposure.

	Control	CNC
IL-1α	1.14 ± 0.03	1.28 ± 0.07*
IL-1β	10.38 ± 0.51	12.15 ± 0.35*
IL-2	2.23 ± 0.10	2.74 ± 0.20*
IL-3	ND	ND
IL-4	ND	ND
IL-5	1.09 ± 0.07	1.25 ± 0.08
IL6	0.05 ± 0.02	0.06 ± 0.02
IL-9	ND	ND
IL-10	5.06 ± 0.21	5.39 ± 0.17
IL-12p40	2.41 ± 0.11	2.56 ± 0.17
IL-12p70	3.63 ± 0.31	9.12 ± 1.19*
IL-13	44.60 ± 3.87	63.28 ± 3.23*
IL-17A	3.07 ± 0.23	3.35 ± 0.17
Eotaxin	94.25 ± 8.41	120.52 ± 15.09
G-CSF	3.10 ± 0.68	3.24 ± 0.74
GM-CSF	ND	ND
IFN-γ	0.06 ± 0.01	0.09 ± 0.02
KC	1.68 ± 0.07	2.63 ± 0.28*
MCP-1	9.39 ± 0.42	11.48 ± 0.35*
MIP-1α	0.46 ± 0.03	0.58 ± 0.06
MIP-1β	4.49 ± 0.09	5.14 ± 0.27
RANTES	0.80 ± 0.05	1.64 ± 0.15*
TNF-α	11.88 ± 0.33	16.43 ± 0.95*

Note. Mice were exposed twice a week for 3 consecutive weeks with a cumulative dose of 240 µg/mouse of CNC and sacrificed 3 mo following their last exposure. Each measurement was assayed in duplicate and normalized by total protein content in testes homogenates. Values are means ± SE (n = 10 mice per group). Asterisk indicates significantly different from controls ($p < .05$). ND corresponds to levels that were below detection limits of the kit.

et al., 2014). Therefore, decreased antioxidant balance and/or low antioxidant enzyme activity in conjunction with accelerated generation of ROS disrupted the physiological functions of spermatozoa, producing impairment of sperm motility and altering sperm morphology (see Figure 7, shown later). Moreover, ROS production has been linked to high frequency of sperm DNA strand breakage (Aitken and Krausz, 2001), base modification, deletions, frame shifts, DNA cross-links, and chromosomal rearrangements (Kemal Duru et al., 2000). Data also demonstrated a significant increase in sperm DNA fragmentation in CNC exposed mice (Figure 2B). The elevation in HNE-His and depletion in GSH levels may be responsible for disruption in the membrane integrity of spermatozoa and may be accountable for decline in sperm DNA integrity (see Figure 7, shown later). Our results are consistent with previously published studies showing a correlation between oxidative stress and changes found in sperm chromatin structure and DNA integrity after exposure to a variety of different nanoparticles (Bungum, 2012; Sycheva et al., 2011; Gromadzka-Ostrowska et al., 2012; Kisin et al., 2014). Moreover, defects in genomic integrity, stability of sperm and DNA repair machineries may trigger arrest of spermatogenesis and abnormal sperm DNA recombination (Agarwal et al., 2014). Similar testicular damage was also reported in other in vivo studies involving exposure to different nanoparticles (Li et al., 2009; Bai et al., 2010). This might account for the significant histopathological alterations found in our study. Interstitial edema, frequent dystrophic seminiferous tubules with arrested spermatogenesis, and degenerating spermatocytes were also detected in the testes of mice exposed to CNC (Figures 4B–4D). The increase in morphological sperm abnormalities, in addition to arrest and impairment of spermatogenesis, presented in this study demonstrate that pulmonary exposure to CNC may lead to male infertility in mice (see Figure 7, shown later). Such changes in various sperm and testes parameters were persistent and extended beyond a full spermatogenic cycle (e.g., 35 d in mice). Data suggest that pulmonary exposure to CNC may critically affect the development/conversion of spermatogonia into spermatids in testes and sperm maturation in epididymis. However, further studies are necessary to delineate the mechanisms underlying CNC-mediated reproductive toxicity in males.

Table 2. Levels (pg/ml) of cytokines, chemokines, and growth factors in the serum following CNC exposure.

	Control	CNC
IL-1α	22.14 ± 1.57	20.65 ± 1.64
IL-1β	247.49 ± 11.69	308.62 ± 23.89*
IL-2	81.75 ± 7.49	112.66 ± 10.07*
IL-3	32.98 ± 2.79	33.65 ± 2.28
IL-4	44.90 ± 3.38	72.51 ± 12.67*
IL-5	37.34 ± 2.21	45.10 ± 3.44
IL6	26.49 ± 2.01	37.24 ± 6.36
IL-9	815.38 ± 92.02	923.40 ± 95.89
IL-10	207.77 ± 15.66	226.57 ± 17.68
IL-12p40	491.76 ± 49.67	703.74 ± 38.88*
IL-12p70	808.71 ± 63.60	856.24 ± 49.87
IL-13	3,105.41 ± 231.04	3718.46 ± 275.08
IL-17A	190.51 ± 11.55	221.67 ± 18.19
Eotaxin	3,542.15 ± 382.92	4744.93 ± 328.68*
G-CSF	222.45 ± 9.30	242.40 ± 9.55
GM-CSF	264.45 ± 9.79	275.30 ± 16.06
IFN-γ	62.74 ± 6.18	77.82 ± 8.33
KC	72.58 ± 4.60	103.31 ± 6.07*
MCP-1	668.04 ± 25.24	776.93 ± 37.65*
MIP-1α	42.68 ± 2.30	43.86 ± 3.44
MIP-1β	59.35 ± 4.03	65.19 ± 3.78
RANTES	51.41 ± 4.34	59.55 ± 7.75
TNF-α	441.98 ± 36.81	569.89 ± 33.30*

Note. Mice were exposed twice a week for 3 consecutive weeks with a cumulative dose of 240 µg/mouse of CNC and sacrificed 3 mo following their last exposure. Each measurement was assayed in duplicate. Values are means ± SE (n = 10 mice per group). Asterisk indicates significantly different from controls ($p < .05$).
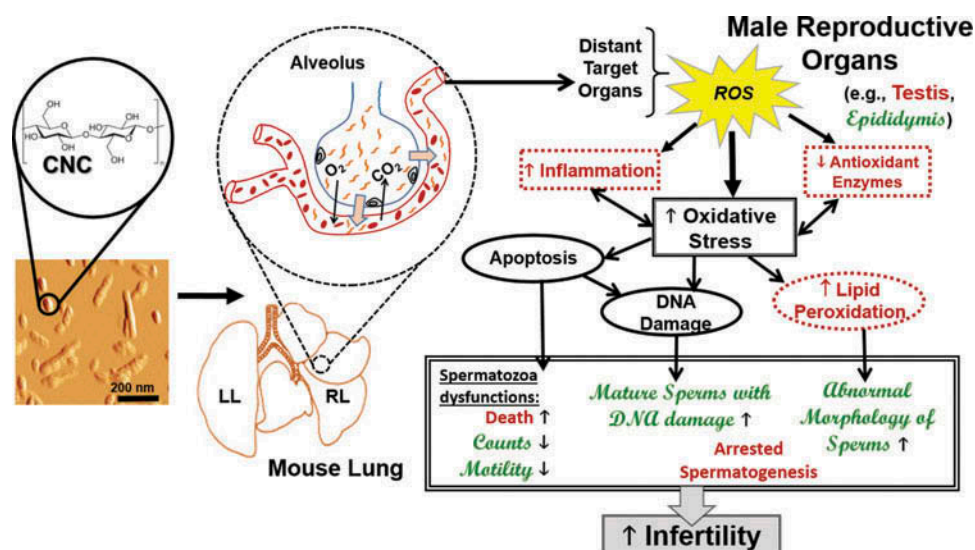
Figure 7. Relationship between various mechanisms and biological effects associated with potential male infertility in mice exposed to CNC via pharyngeal aspiration. The schema proposes the extrapulmonary translocation of CNC particles to distant organs and briefly illustrates how enhanced oxidative stress can cause changes at different levels of male reproductive organs, leading to male infertility. The precise mechanisms that are modulated or perturbed in the testis and in the epididymis of CNC-exposed mice are highlighted in Arial red font and Script MT green font, respectively.

Over the past several years, a number of studies focused on the interplay of cytokines, chemokines and growth factors and their relationship to male reproductive physiology (Fraczek and Kurpisz, 2015). Different studies reported that cytokines (IL-1α, IL-1β, Il-6, IL-8, IL-12, and TNF-α) are involved in the regulation of spermatogenesis, semen quality, and male reproductive tract pathological conditions (Eggert-Kruse et al., 2001; Papadimas et al., 2002; Sanocka et al., 2003). However, the nature, origin, and role of different cytokines in

the male reproductive tract are not yet clearly understood (Fraczek and Kurpisz, 2015). Cytokine levels are interconnected with multiple factors, including steroid hormones, the redox system, and prostaglandins (Ochsendorf, 1999; Huleihel and Lunenfeld, 2004). Sanocka et al. (2003) suggested that proinflammatory cytokines released into the seminal plasma during male genital tract inflammation might modify the activity of the pro-oxidative and antioxidative balance, thus leading to oxidative stress and sustained damage of spermatozoa. Evidence suggests that increased levels of proinflammatory cytokines, including TNF-α, IL-1α, and IL-1β, might affect sperm function by induction of apoptosis. Previously, it was reported that elevated levels of TNF-α, IL-1α, and IL-1β were associated with reduced sperm count, motility, and sperm morphology (Perdichizzi et al., 2007; Gruschwitz et al., 1996). Our data demonstrated that pulmonary exposure to CNC induced significant upregulation of five proinflammatory cytokines (IL-1α, IL-1β, IL-2, IL-12p70, and TNF-α) and three proinflammatory chemokines (KC, MCP-1, and RANTES) in mouse testes (Table 1). These results are associated with increase in oxidative damage (HNE-His, GSH) and inflammatory marker (MPO) present in testes, atypical sperm parameters (sperm number, motile and morphologically normal cells), and sperm DNA integrity (Figures 1-3, 6). Several in vitro experimental studies showed a correlation between proinflammatory cytokines and significant loss of sperm genomic integrity (Fraczek et al., 2013). The induction of sperm membrane injury and sperm DNA damage may be produced by mechanisms where proinflammatory cytokines affect spermatozoa (Fraczek et al., 2013). In addition, the anti-inflammatory cytokine IL-13 plays an important role in maintaining an immunosuppressive and anti-inflammatory environment and is essential for sperm development (Maresz et al., 2008). In our study, a significant accumulation of IL-13 was observed in testes after exposure to CNC, perhaps imposing pathway activation through mechanisms upholding wound healing, which

is vital for normal testes functions (Maresz et al., 2008).

Testosterone and LH are two essential hormones required for growth, reproduction, health, and well-being in men. However, several studies suggested that testosterone possesses pro-oxidant properties (Royle et al., 2001; Gil et al., 2004), and excessive levels might trigger oxidation in testicular tissues noted in mice, rats, and rabbits (Peltola et al., 1996; Chainy et al., 1997; Kisin et al., 2014; Aydilek et al., 2004). Disruption of normal hormone levels were also observed in previous in vivo studies that investigated effects of exposure to other nanoparticles (Li et al., 2009; 2012; 2013; Yoshida et al., 2009; Yamagishi et al., 2012; Kisin et al., 2014). Similarly, exposure to CNC was found to enhance testosterone levels in testes and serum (Figure 5A and 5B), while levels of LH were lowered in serum (Figure 5C). These findings may be attributed to hypothalamo–pituitary–gonadal feedback system (Kamel and Kubajak, 1987). In the testes, LH binds to its receptor on Leydig cells to initiate testosterone production. High levels of testosterone (i.e., hypertestosteronism) suppress gonadotropin-releasing hormone discharge from the hypothalamus, thus negatively regulating production of LH (Alonso-Alvarez et al., 2007), and consequentially resulting in decreased sperm production.

The responses after CNC exposure found in serum were less pronounced compared to inflammation observed in testes. Choi et al. (2010) reported rapid extrapulmonary distribution and translocation of chitosan nanoparticles to various distant organs, including the interstitium of testes, following intra-tracheal instillation. Based on the chemical resemblance of chitosan to cellulose (Martínez and Gozalbo, 2001), it is conceivable that responses found in male reproductive organs of mice exposed to CNC may also be due to direct translocation of nanoparticles to testes. The schema illustrating the possible relationship between various mechanisms associated with extrapulmonary translocation of CNC particles enhancing oxidative stress responses that are potentially leading to male infertility is presented in Figure 7.

Funding

Disclaimer

The findings and conclusions in this report are those of the authors and do not necessarily represent the views of the National Institute for Occupational Safety and Health.

Conflict of Interest

No conflict of interest relevant to this article is present.

References

Agarwal, A., Durairajanayagam, D., Halabi, J., Peng, J., and Vazquez-Levin, M. 2014. Proteomics, oxidative stress and male infertility. *Reprod. BioMed. Online* 29: 32–58.

Aitken, R. J., and Krausz, C. 2001. Oxidative stress, DNA damage and the Y chromosome. *Reproduction* 122: 497–506.

Aitken, R. J., and Roman, S. D. 2008. Antioxidant systems and oxidative stress in the testes. *Oxidat Med Cell Longevity* 1: 15–24.

Alonso-Alvarez, C., Bertrand, S., Faivre, B., Chastel, O., and Sorci, G. 2007. Testosterone and oxidative stress: The oxidation handicap hypothesis. *Proc. R. Soc. London B Biol. Sci.* 274: 819–825.

Aydilek, N., Aksakal, M., and Karakilcik, A. Z. 2004. Effects of testosterone and vitamin E on the antioxidant system in rabbit testis. *Andrologia* 36: 277–281.

Bai, Y., Zhang, Y., Zhang, J., Mu, Q., Zhang, W., Butch, E. R., Snyder, S. E., and Yan, B. 2010. Repeated administrations of carbon nanotubes in male mice cause reversible testis damage without affecting fertility. *Nat. Nanotechnol.* 5: 683–689.

Brown, E. E., Hu, D., Abu Lail, N., and Zhang, X. 2013. Potential of nanocrystalline cellulose–fibrin nanocomposites for artificial vascular graft applications. *Biomacromolecules* 14: 1063–1071.

Bungum, M. 2012. Sperm DNA integrity assessment: A new tool in diagnosis and treatment of fertility, obstetrics and gynecology. *Obstet. Gynecol. Int.* 2012: article ID 531042.

Buzea, C., Pacheco, I. I., and Robbie, K. 2007. Nanomaterials and nanoparticles: Sources and toxicity. *Biointerphases* 2: MR17–71.

Catalan, J., Ilves, M., Jarventaus, H., Hannukainen, K. S., Kontturi, E., Vanhala, E., Alenius, H., Savolainen, K. M., and Norppa, H. 2015. Genotoxic and immunotoxic effects of cellulose nanocrystals *in vitro*. *Environ. Mol. Mutagen.* 56:171–182.

Chainy, G. B., Samantaray, S., and Samanta, L. 1997. Testosterone-induced changes in testicular antioxidant system. *Andrologia* 29: 343–349.

Cherian, B. M., Leao, A. L., de Souza, S. F., Thomas, S., Pothan, L. A., and Kottaisamy, M. 2011. Cellulose nanocomposites for high-performance applications. In *Cellulose fibers: Bio- and nano-polymer composites*, ed. S. Kalia, B. S. Kaith, and I. Kaur, 539–587. Berlin, Germany: Springer.

Choi, M., Cho, M., Han, B. S., Hong, J., Jeong, J., Park, S., Cho, M. H., Kim, K., and Cho, W. S. 2010. Chitosan nanoparticles show rapid extrapulmonary tissue distribution and excretion with mild pulmonary inflammation to mice. *Toxicol. Lett.* 199: 144–152.

Clift, M. J., Foster, E. J., Vanhecke, D., Studer, D., Wick, P., Gehr, P., Rothen-Rutishauser, B., and Weder, C. 2011. Investigating the interaction of cellulose nanofibers derived from cotton with a sophisticated 3D human lung cell coculture. *Biomacromolecules* 12: 3666–3673.

Cyphert, J. M., McGee, M. A., Nyska, A., Schladweiler, M. C., Kodavanti, U. P., Gavett, S. H. 2016. Long-term toxicity of naturally occurring asbestos in male Fischer 344 rats. *J. Toxicol. Environ. Health A* 79: 49–60.

Eggert-Kruse, W., Boit, R., Rohr, G., Aufenanger, J., Hund, M., and Strowitzki, T. 2001. Relationship of seminal plasma interleukin (IL)-8 and IL-6 withsemen quality. *Hum. Reprod.* 16: 517–528.

Evenson, D. P. 2013. Sperm chromatin structure assay (SCSA®). *Methods Mol. Biol.* 927: 147–164.

Fraczek, M., and Kurpisz, M. 2015. Mechanisms of the harmful effects of bacterial semen infection on ejaculated human spermatozoa: Potential inflammatory markers in semen. *Folia Histochem. Cytobiol.* 53: 201–217.

Fraczek, M., Szumala-Kakol, A., Dworacki, G., Sanocka, D., and Kurpisz, M. 2013. In vitro reconstruction of inflammatory reaction in human semen: Effect on sperm DNA fragmentation. *J. Reprod. Immunol.* 100: 76–85.

Gil, D., Heim, C., Bulmer, E., Rocha, M., Puerta, M., and Naguib, M. 2004. Negative effects of early developmental stress on yolk testosterone levels in a passerine bird. *J. Exp. Biol.* 207: 2215–2220.

Goldman, L., and Coussens, C. 2005. *Implications of nanotechnology for environmental health research*, Vol. 4, *Nanotechnology: Government involvement.* Washington, DC: National Academies Press.

Greil, A. L., Slauson-Blevins, K., and McQuillan, J. 2010. The experience of infertility: A review of recent literature. *Sociol. Health Illness* 32: 140–162.

Griveau, J. F., Dumont, E., Renard, P., Callegari, J. P., and Le Lannou, D. 1995. Reactive oxygen species, lipid peroxidation and enzymatic defence systems in human spermatozoa. *J. Reprod. Fertil.* 103: 17–26.

Gromadzka-Ostrowska, J., Dziendzikowska, K., Lankoff, A., Dobrzyńska, M., Instanes, C., Brunborg, G., Gajowik, A., Radzikowska, J., Wojewódzka, M., and Kruszewski, M. 2012. Silver nanoparticles effects on epididymal sperm in rats. *Toxicol. Lett.* 214: 251–258.

Gruschwitz, M. S., Brezinschek, R., and Brezinschek, H. P. 1996. Cytokine levels in the seminal plasma of infertile males. *J. Androl.* 17: 158–163.

Guo, L.L., Liu, X. H., Qin, D. X., Gao, L., Zhang, H. M., Liu, J. Y., and Cui, Y. G. 2009. Effects of nanosized titanium dioxide on the reproductive system of male mice. *Zhonghua Nan Ke Xue* 15: 517–522.

Huleihel, M., and Lunenfeld, E. 2004. Regulation of spermatogenesis by paracrine/autocrine testicular factors. *Asian J. Androl.* 6: 259–268.

Iavicoli, I., Fontana, L., Leso, V., and Bergamaschi, A. 2013. The effects of nanomaterials as endocrine disruptors. *Int. J. Mol. Sci.* 14: 16732–16801.

Iommiello, V. M., Albani, E., Di Rosa, A., Marras, A., Menduni, F., Morreale, G., Levi, S. L., Pisano, B., and Levi-Setti, P. E. 2015. Ejaculate oxidative stress is related with sperm DNA fragmentation and round cells. *Int. J. Endocrinol.* 2015: 321901.

Jouannet, P., Wang, C., Eustache, F., Kold-Jensen, T., and Auger, J. 2001. Semen quality and male reproductive health: The controversy about human sperm concentration decline. *Acta Pathol. Microbiol. Immunol. Scand.* 109: 333–344.

Kamel, F., and Kubajak, C. L. 1987. Modulation of gonadotropin secretion by corticosterone: Interaction with gonadal steroids and mechanism of action. *Endocrinology* 121: 561–568.

Kermanizadeh, A., Gosens, I., MacCalman, L., Johnston, H., Danielsen, P. H., Jacobsen, N. R., Lenz, A. G., Fernandes, T., Schins, R. P., Cassee, F. R., Wallin, H., Kreyling, W., Stoeger, T., Loft, S., M. Ã., ller, P., Tran, L., and Stone, V. 2016. A multilaboratory toxicological assessment of a panel of 10 engineered nanomaterials to human health—ENPRA Project—The highlights, limitations, and current and future challenges. *J. Toxicol. Environ. Health B* 19: 1–28.

Kisin, E. R., Yanamala, N., Farcas, M. T., Gutkin, D. W., Shurin, M. R., Kagan, V. E., Bugarski, A. D., and Shvedova, A. A. 2014. Abnormalities in the male reproductive system after exposure to diesel and biodiesel blend. *Environ. Mol. Mutagen.* 56: 265–276.

Knight, J. A., and Marrett, L. D. 1997. Parental occupational exposure and the risk of testicular cancer in Ontario. *J. Occup. Environ. Med.* 39: 333–338.

Kodama, H., Kuribayashi, Y., and Gagnon, C. 1996. Effect of sperm lipid peroxidation on fertilization. *J. Androl.* 17: 151–157.

Li, C., Taneda, S., Taya, K., Watanabe, G., Li, X., Fujitani, Y., Ito, Y., Nakajima, T., and Suzuki, A. K. 2009. Effects of inhaled nanoparticle-rich diesel exhaust on regulation of testicular function in adult male rats. *Inhal. Toxicol.* 21:803–811.

Li, C., Li, X., Jigami, J., Hasegawa, C., Suzuki, A. K., Zhang, Y., Fujitani, Y., Nagaoka, K., Watanabe, G., and Taya, K. 2012. Effect of nanoparticle-rich diesel exhaust on testosterone biosynthesis in adult male mice. *Inhal. Toxicol.* 24:599–608.

Li, W. Q., Wang, F., Liu, Z. M., Wang, Y. C., Wang, J., and Sun, F. 2013. Gold nanoparticles elevate plasma testosterone levels in male mice without affecting fertility. *Small* 27: 1708–1714.

Liu, Y., Li, H., and Xiao, K. 2016. Distribution and biological effects of nanoparticles in the reproductive system. *Curr. Drug Metab.* 17:478–496

Makker, K., Agarwal, A., and Sharma, R. 2009. Oxidative stress and male infertility. *Indian J. Med. Res.* 129: 357–367.

Maresz, K., Ponomarev, E. D., Barteneva, N., Tan, Y., Mann, M. K., and Dittel, B. N. 2008. IL-13 induces the expression of the alternative activation marker Ym1 in a subset of testicular macrophages. *J. Reprod. Immunol.* 78:140–148.

Martínez, J. P., and Gozalbo, D. 2001. Chitin. In *eLS*. John Wiley & Sons.

Masella, R., Di Benedetto, R., Vari, R., Filesi, C., and Giovannini, C. 2005. Novel mechanisms of natural antioxidant compounds in biological systems: Involvement of glutathione and glutathione-related enzymes. *J. Nutr. Biochem.* 16: 577–586.

Oberdörster, G., Castranova, V., Asgharian, B., and Sayre, P. 2015. Inhalation exposure to carbon nanotubes (CNT) and carbon nanofibers (CNF): Methodology and dosimetry. *J. Toxicol. Environ. Health B* 18: 121–212.

Ochsendorf, F. R. 1999. Infections in the male genital tract and reactive oxygen species. *Hum. Reprod. Update* 5: 399–420.

Oliva, A., Spira, A., and Multigner, L. 2001. Contribution of environmental factors to the risk of male infertility. *Hum. Reprod. Update* 16: 1768–1776.

Papadimas, J., Goulis, D. G., Sotiriades, A., Daniilidis, M., Fleva, A., Bontis, J. N., and Tourkantonis, A. 2002. Interleukin-1 beta and tumor necrosis factor-alpha innormal/infertile men. *Arch. Androl.* 48: 107–113.

Peltola, V., Huhtaniemi, I., Metsa-Ketela, T., and Ahotupa, M. 1996. Induction of lipid peroxidation during steroidogenesis in the rat testis. *Endocrinology* 137: 105–112.

Peng, B. L., Dhar, N., Liu, H. L., and Tam, K. C. 2011. Chemistry and applications of nanocrystalline cellulose and its derivatives: A nanotechnology perspective. *Can. J. Chem. Eng.* 89: 1191–1206.

Perdichizzi, A., Nicoletti, F., La Vignera, S., Barone, N., D'Agata, R., Vicari, E., and Calogero, A. E. 2007. Effects of tumour necrosis factor-alpha on human sperm motility and apoptosis. *J. Clin. Immunol.* 27:152–162.

Pereira, M. A., Sabharwal, P. S., Gordon, L., and Wyrobek, A. J. 1981. The effect of diesel exhaust on sperm-shape abnormalities in mice. *Environ. Int.* 5: 459–460.

Phillips, K. P., and Tanphaichitr, N. 2008. Human exposure to endocrine disrupters and semen quality. *J. Toxicol. Environ. Health B* 11: 188–220.

Rajesh Kumar, T., Doreswamy, K., Shrilatha, B., and Muralidhara. 2002. Oxidative stress associated DNA damage in testis of mice: Induction of abnormal sperms and effects on fertility. *Mutat. Res.* 513: 103–111.

Royle, N. J., Surai, P. F., and Hartley, I. R. 2001. Maternally derived androgens and antioxidants in bird eggs: Complementary but opposing effects? *Behav. Ecol.* 12:381–385.

Sanocka, D., Jedrzejczak, P., Szumala-Kaekol, A., Fraczek, M., and Kurpisz, M. 2003. Male genital tract inflammation: The role of selected interleukins in regulation of pro-oxidant and antioxidant enzymatic substances in seminal plasma. *J. Androl.* 24: 448–455.

Sharlip, I. D., Jarow, J. P., Belker, A. M., Lipshultz, L. I., Sigman, M., Thomas, A. J., Schlegel, P. N., Howards, S. S., Nehra, A., Damewood, M. D., Overstreet, J. W., and Sadovsky, R. 2002. Best practice policies for male infertility. *Fertil. Steril.* 77: 873–882.

Shrilatha, B., and Muralidhara, D. 2007. Early oxidative stress in testis and epididymal sperm in streptozotocin-induced diabetic mice: Its progression and genotoxic consequences. *Reprod. Toxicol.* 23: 578–587.

Shvedova, A. A., Yanamala, N., Kisin, E. R., Tkach, A. V., Murray, A. R., Hubbs, A., Chirila, M. M., Keohavong, P., Sycheva, L. P., Kagan, V. E., and Castranova, V. 2014. Long-term effects of carbon containing engineered nanomaterials and asbestos in the lung: One year postexposure comparisons. *Am. J. Physiol. Lung Cell Mol. Physiol.* 306: L170–L182.

Shvedova, A. A., Kisin, E. R., Yanamala, N., Farcas, M. T., Menas, A. L., Fournier, P., Reynolds, J. S., Gutkin, D., Star, A., Reiner, R., Halappanavar, S., and Kagan, V. E. 2016. Gender differences in murine pulmonary responses elicited by nano-crystalline cellulose. *Part. Fibre Toxicol.* 13: 28

Snyder-Talkington, B. N., Dong, C., Porter, D. W., Ducatman, B., Wolfarth, M. G., Andrew, M., Battelli, L., Raese, R., Castranova, V., Guo. N. L., and Qian, Y. 2016. Multiwalled carbon nanotube-induced pulmonary inflammation and fibrotic responses and genomic changes following aspiration exposure in mice: A 1-year postexposure study. *J. Toxicol. Environ. Health A* 79: 352–366.

Stefaniak, A. B., Seehra, M. S., Fix, N. R., and Leonard, S. S. 2014. Lung biodurability and free radical production of cellulose nanomaterials. *Inhal. Toxicol.* 26: 733–749.

Sycheva, L. P., Zhurkov, V. S., Iurchenko, V. V., Daugel-Dauge, N. O., Kovalenko, M. A., Krivtsova, E. K., and Durnev, A. D. 2011. Investigation of genotoxic and cytotoxic effects of micro- and nanosized titanium dioxide in six organs of mice *in vivo*. *Mutat. Res.* 726: 8–14.

Wegner, T. H., Ireland, S., and Jones, J. P. E. 2013. Cellulosic nanomaterials: Sustainable materials of choice for the 21st century. In *Production and applications of cellulose nanomaterials*, ed. M. T. Postek, R. J. Moon, A. W. Rudie, and M. A. Bilodeau, 3–8. Peachtree Corners, GA: TAPPI Press.

Yamagishi, N., Ito, Y., Ramdhan, D. H., Yanagiba, Y., Hayashi, Y., Wang, D., Li, C. M., Taneda, S., Suzuki, A. K., Taya, K., Watanabe, G., Kamijima, M., and Nakajima, T. 2012. Effect of nanoparticle-rich diesel exhaust on testicular and hippocampus steroidogenesis in male rats. *Inhal. Toxicol.* 24: 459–467.

Yanamala, N., Farcas, M. T., Hatfield, M. K., Kisin, E. R., Kagan, V. E., Geraci, C. L., and Shvedova, A. A. 2014. In vivo evaluation of the pulmonary toxicity of cellulose nanocrystals: A renewable and sustainable nanomaterial of the future. *ACS Sustain. Chem. Eng.* 2: 1691–1698.

Yoshida, S., Hiyoshi, K., Ichinose, T., Takano, H., Oshio, S., Sugawara, I., Takeda, K., and Shibamoto, T. 2009. Effect of nanoparticles on the male reproductive system of mice. *Int J. Androl.* 32: 337–342.

Zhang, M., Ding, C., Yang, J., Lin, S., Chen, L., and Huang, L. 2016. Study of interaction between water-soluble collagen and carboxymethyl cellulose in neutral aqueous solution. *Carbohydr. Polym.* 137: 410–417.